Appl Phys A (2010) 100: 79–82
DOI 10.1007/s00339-010-5796-8

Applied Physics A
Materials Science & Processing

RAPID COMMUNICATION

Magnetic properties of Er-doped ZnO films prepared by reactive magnetron sputtering

Jing Qi · Daqiang Gao · Jinhong Liu · Wenge Yang · Qi Wang · Jinyuan Zhou · Yinghu Yang · Jianlin Liu

Received: 17 February 2010 / Accepted: 19 May 2010 / Published online: 5 June 2010

Abstract All $Zn_{1-x}Er_xO$ ($x = 0.04$, 0.05, and 0.17) films deposited on glass substrates by radio-frequency reactive magnetron sputtering exhibit the mixture of ferromagnetic and paramagnetic phases at room temperature. The estimated magnetic moment per Er ion decreases with the increase of Er concentration. The temperature dependence of the magnetization indicates that there is no intermetallic ErZn buried in the films. The ferromagnetism is attributed to the Er ions substitution for Zn^{2+} in ZnO lattices, and it can be interpreted by the bound-magnetic-polaron model.

In semiconductor devices, one usually takes advantage of the charge of electrons. In contrast, magnetic materials are utilized on the basis of electron spin. In order to develop new electronics, it is necessary to combine both features. Diluted magnetic semiconductor (DMS) can serve as an avenue to utilize both charge and spin functions of electrons for various applications [1]. Many group IV [2], III–V [3], and II–VI [3] DMS materials have been obtained by doping magnetic impurities into semiconductors. Nevertheless, most of them have a low Curie temperature (T_C), which limits their practical applications. In the quest for materials with high T_C, the wide-gap material, ZnO, has emerged as an attractive candidate based on both theoretical and experimental studies for integrating the optical, electronic, and magnetic properties into a single substance [4, 5]. So far, room temperature (RT) ferromagnetism (FM) has been reported in many transition metal doped ZnO such as those doped with Mn [6], Co [7], Cr [8], Ni [9], V [10], Fe [11], and Gd [12]. On the other hand, characteristics of erbium doped ZnO thin films have been widely studied, such as the structural characteristics [13], optical properties [14], and electrical properties [15]. Nevertheless, the magnetic properties of Er-doped ZnO materials have seldom been reported. In this paper, the magnetic properties of a series of Er-doped ZnO thin films are studied and the origin of FM is also discussed.

The transparent Er-doped ZnO films were grown on glass substrates by radio-frequency (RF) reactive magnetron sputtering using Zn (purity: 99.99%) and Er (purity: 99.996%) together as targets. The sputtering chamber was evacuated by a molecular pump to a base pressure below 2×10^{-5} Pa. During sputtering, the substrate temperature was kept at RT. Oxygen was introduced into the chamber as the reactive gas and the flow rate was controlled at 20, 25, 30, and 35 sccm, respectively. Additionally, argon was introduced into the chamber as working gas and its flow rate was regulated at 15 sccm. During the deposition, the chamber pressure and sputter power were fixed at 2.0 Pa and 5.3 W/cm^2, respectively. The as-grown samples are denoted as $Zn_{1-x}Er_xO$. Magnetic measurements were performed by vibrating sample magnetometer (VSM) and superconducting quantum interference device (SQUID), where the magnetic fields were parallel to the film planes. X-ray photoelectron spectroscopy (XPS) was used to analyze chemical valences and chemical compositions of the films.

J. Qi (✉) · D. Gao · J. Liu · W. Yang
The Key Laboratory for Magnetism and Magnetic Materials of MOE, Lanzhou University, Lanzhou 730000, China
e-mail: qijing@lzu.edu.cn
Fax: 86-931-8913554

J. Qi · Q. Wang · J. Zhou · Y. Yang
Department of Physics, School of Physical Science and Technology, Lanzhou University, Lanzhou 730000, China

J. Qi · J. Liu
Quantum Structures Laboratory, Department of Electrical Engineering, University of California at Riverside, Riverside, CA 92521, USA

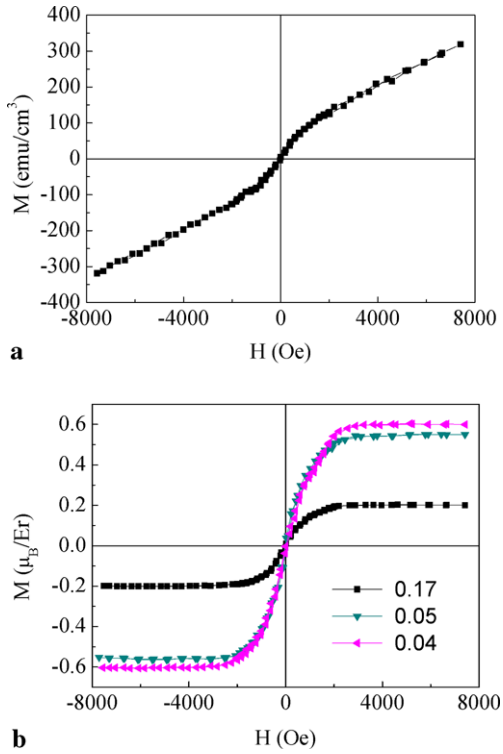

Fig. 1 (**a**) M–H curve of the $Zn_{0.96}Er_{0.04}O$ film measured at RT, which were deposited at RT on glass substrates with O_2 flow rate of 35 sccm. (**b**) M–H curves measured at RT for $Zn_{1-x}Er_xO$ ($x = 0.04$, 0.05, and 0.17), in which the contribution of the paramagnetism in the films and the holder of VSM was deducted

The samples were prepared and handled carefully to avoid any possible magnetic contamination. The undoped ZnO films prepared under the same conditions were examined and showed nonferromagnetic behavior, confirming that there is no extrinsic magnetic impurity contamination during the procedure of preparation. Figure 1(a) shows the M–H curve of the $Zn_{0.96}Er_{0.04}O$ sample, which was deposited at RT with O_2 flow rate of 35 sccm. The measurement was carried out at RT by VSM under a maximum applied magnetic field of 8 kOe. The curve is composed of two parts: at lower field ($H \leq 2000$ Oe), the curve exhibits magnetic hysteresis with a magnetic moment of 33 emu/cm^{-3} and coercivity of 28 Oe; while at higher field ($H \geq 2000$ Oe), the curve exhibits paramagnetic behavior. Figure 1(b) shows the magnetization versus magnetic field (M–H) curves measured at RT for $Zn_{1-x}Er_xO$ ($x = 0.04$, 0.05, and 0.17), where the contributions of the paramagnetism from both the films and the holder of VSM were deducted. As the Er concentration increases, the magnetic moment per erbium ion decreases from $0.60\mu_B$/Er ($x = 0.04$) to $0.20\mu_B$/Er ($x = 0.17$). The consistent drop in moment per Er ion at higher Er concentration could be due to an increasing occurrence of antiferromagnetic coupling between Er pairs occurring at shorter separation distances, which was similar to the system of Cu-doped ZnO [16].

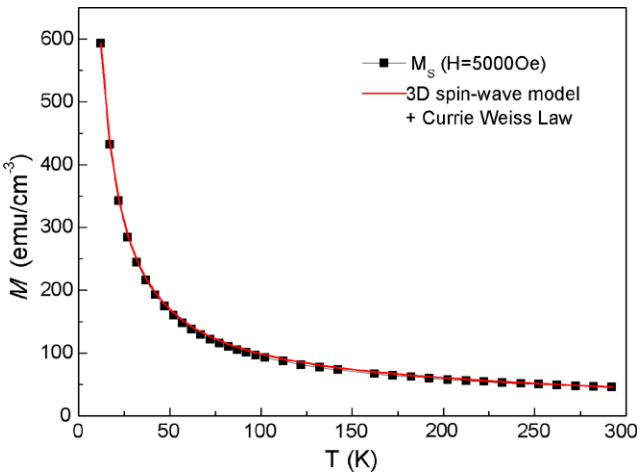

Fig. 2 M–T curve in field of 5000 Oe for $Zn_{0.96}Er_{0.04}O$ film deposited at RT with O_2 flow rate of 35 sccm on glass substrate. The fitting result is shown as the *solid curve*

The temperature dependence of magnetization (M–T) was measured by SQUID from 5 to 300 K in the field of 5000 Oe for the $Zn_{0.96}Er_{0.04}O$ film, which is shown in Fig. 2. Neither standard 3D spin-wave model nor the Curie–Weiss model can fit the $M(T)$ data unless both models are taken into account, i.e. [17]

$$M(T) = \frac{CH}{T - \theta_p} + M(0)(1 - AT^{3/2}),$$

where $M(0)$ is the saturation magnetization at $T = 0$ K, and A is a coefficient correlated with the structural properties of material, C is the Curie constant and θ_p is the paramagnetic Curie temperature. The best fit for the sample is shown by solid curve in Fig. 2, from which we obtain $M(0) = 29.5$ emu/cm^{-3}, $C = 1.42$ emu K/cm^3·Oe and $\theta_p = -0.596$ K. The good fit of the combination of the standard 3D spin-wave and Curie–Weiss model suggests the coexistence of ferromagnetic and paramagnetic phases in the film. Temperature dependence of the magnetization also indicates that there is no intermetallic ErZn because there is no kink at $T_C \sim 20$ K in the M–T plot. [18]

Figure 3 shows XPS survey spectrum of the $Zn_{0.96}Er_{0.04}O$ film prepared at the O_2 flow rate of 35 sccm. The result indicates that no other metal ions other than Zn and Er can be detected, and that Er ions are in a trivalent state in the $Zn_{0.96}Er_{0.04}O$ film. XPS measurements of other $Zn_{1-x}Er_xO$ films led to similar spectra. Therefore, we can conclude that the RT FM is an intrinsic property of the materials caused by the presence of erbium in high-spin configuration ($4f^{11}6s^0$). The XPS result of the $Zn_{0.96}Er_{0.04}O$ sample also gives the fact that the atomic ratio of (Er + Zn) and O is about 2:5.

To further understand the origin of the FM of the films, the influence of O_2 flow rate on the ferromagnetic proper-

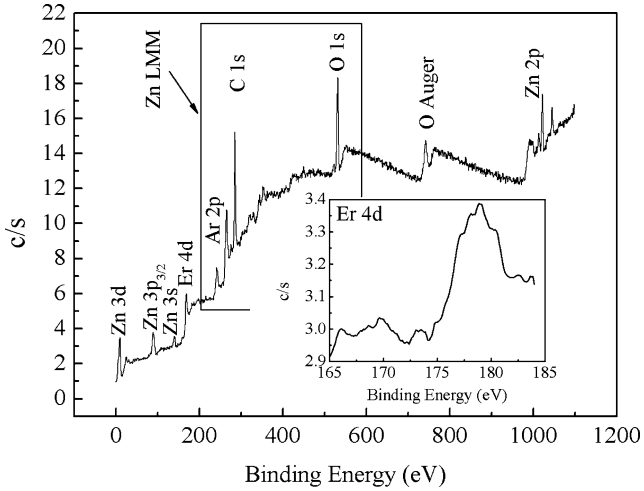

Fig. 3 XPS survey spectrum for $Zn_{0.96}Er_{0.04}O$ thin films. *Inset*: high resolution scan of Er 4d

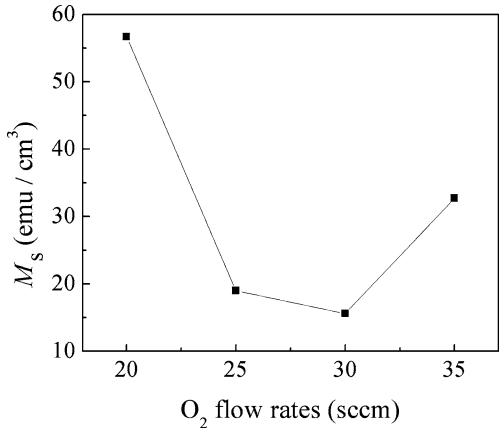

Fig. 4 M_S values versus O_2 flow rate in the $Zn_{0.96}Er_{0.04}O$ films

ties is studied. Figure 4 shows the RT saturation magnetization as a function of O_2 flow rate for $Zn_{0.96}Er_{0.04}O$. As the O_2 flow rate decreases from 35 to 25 sccm, there is a drastic reduction in M_S values. Further decrease of O_2 flow rate from 25 sccm to 20 sccm results in an evident increase in M_S. It has been reported that dopants such as Sb [19] and Cu [20] in ZnO can increase the number of point defects. Meanwhile, Kohan et al. [21] calculated formation energies and electronic structure of native point defects in ZnO by using the first-principle pseudopotential method. Their calculation results showed that, depending on the partial pressure of Zn, the two most common defects in ZnO are likely to be oxygen and zinc vacancies (V_O, and V_{Zn}). In particular, V_O has lower formation energy than the zinc interstitial and hence should be more abundant in Zn-rich conditions; and correspondingly, V_{Zn} should dominate in O-rich conditions. So, it is reasonable to conclude that abundant zinc vacancies and oxygen vacancies may exist in the Er-doped ZnO films deposited at the O_2 flow rates of 35 sccm and 20 sccm, respectively. Our experimental results may be consistent with bound-magnetic-polaron (BMP) model proposed by Coey et al. [22], since both zinc and oxygen vacancies favor the formation of FM in DMS [23, 24]. The magnetic exchange interaction between Zn or O vacancies and Er^{3+} ions occupying the same space are aligned with Er^{3+} spins, forming BMPs. With the reduction of zinc or oxygen vacancies by changing O_2 flow rates, neighboring Er ions coupled via a zinc or oxygen vacancy (ferromagnetic exchange) are now coupled by a zinc bond (no exchange interaction) or oxygen bond (superexchange interaction), which are responsible for the drastic alteration in M_S values.

In summary, Er-doped ZnO thin films have been grown on glass substrates by RF magnetron reactive co-sputtering with Zn and Er targets. The experimental results indicate that Er-doped ZnO thin films are the mixture of ferromagnetic and paramagnetic phases at RT. Er ions are in trivalent state in the $Zn_{1-x}Er_xO$ thin films. FM in the films is caused by the substitution of Zn^{2+} in ZnO lattice by Er^{3+} ions. The estimated magnetic moment per Er atom decreases with the erbium concentration increase. The result is due to an increase in the number of erbium ions occupying adjacent cation lattice positions, which are antiferromagnetic coupled with each other. The increase of O_2 flow rate from 20 sccm to 35 sccm, which changed the type and concentration of defects in the films, leads to the alteration of the magnetic moment in Er-doped ZnO films. This suggests that an exchange mechanism associated with defects such as oxygen and zinc vacancies is responsible for the FM in the $Zn_{1-x}Er_xO$ thin films.

Acknowledgements Financial supports by National Natural Science Foundation of China (No. 50902065) and Science and Technology Projects of Gansu Province (No. 0710RJZA023) are appreciated. The research at UCR was supported by DOD/DMEA through the center of Nanomaterials and Nanodevices (CNN) and the award No. H9403-08-2-0803.

References

1. J.K. Furdyna, J. Appl. Phys. **64**, 29 (1988)
2. M. Bolduc, C. Awo-Affouda, A. Stollenwerk, M.B. Huang, F.G. Ramos, G. Agnello, V.P. LaBella, Phys. Rev. B **71**, 033302 (2005)
3. T. Dietl, H. Ohno, Mater. Res. Soc. Bull. **28**, 714 (2003)
4. A. Quesada, M.A. García, J. de la Venta, E. Fernández Pinel, J.M. Merino, A. Hernando, Eur. Phys. J. B **59**, 457 (2007)
5. K. Sato, H. Katayama-Yoshida, Jpn. J. Appl. Phys. **39**, L555 (2000)
6. Z. Yang, W.P. Beyermann, M.B. Katz, O.K. Ezekoye, Z. Zuo, Y. Pu, J. Shi, X.Q. Pan, J.L. Liu, J. Appl. Phys. **105**, 053708 (2009)
7. Z. Yang, M. Biasini, W.P. Beyermann, M.B. Katz, O.K. Ezekoye, X.Q. Pan, Y. Pu, J. Shi, Z. Zuo, J.L. Liu, J. Appl. Phys. **104**, 113712 (2008)

8. Y.C. Yang, C.F. Zhong, X.H. Wang, B. He, S.Q. Wei, F. Zeng, F. Pan, J. Appl. Phys. **104**, 064102 (2008)
9. H. Wang, Y. Chen, H.B. Wang, C. Zhang, F.J. Yang, J.X. Duan, C.P. Yang, Y.M. Xu, M.J. Zhou, Q. Li, Appl. Phys. Lett. **90**, 052505 (2007)
10. N.H. Hong, J. Sakai, A. Hassini, J. Phys., Condens. Matter **17**, 199 (2005)
11. B. Zhang, Q.H. Li, L.Q. Shi, H.S. Cheng, J.Z. Wang, J. Vac. Sci. Technol. A **26**, 1469 (2008)
12. K. Potzger, S. Zhou, F. Eichhorn, M. Helm, W. Skorupa, A. Mücklich, J. Fassbender, T. Herrmannsdörfer, A. Bianchi, J. Appl. Phys. **99**, 063906 (2006)
13. R.P. Casero, A.G. Llorente, O. Pons-Y-Moll, W. Seller, R.M. Defourneau, D. Defourneau, E. Millon, J. Perriere, P. Goldner, B. Viana, J. Appl. Phys. **97**, 054905 (2005)
14. Z. Pan, S.H. Morgan, A. Ueda, A. Aga Jr., A. Steigerwald, A.B. Hmelo, R. Mu, J. Phys., Condens. Matter **19**, 266216 (2007)
15. D. Dimova-Malinovska, H. Nichev, O. Angelov, V. Grigorov, M. Kamenova, Superlattices Microstruct. **42**, 123 (2007)
16. D. Chakraborti, G.R. Trichy, J.T. Prater, J. Narayan, J. Phys. D, Appl. Phys. **40**, 7606 (2007)
17. L. Zhang, S. Ge, Y. Zuo, X. Zhou, Y. Xiao, S. Yan, X. Han, Z. Wen, J. Appl. Phys. **104**, 123909 (2008)
18. P. Morin, J. Rouchy, E. du Tremolet de Lacheisserie, Phys. Rev. B **16**, 3182 (1977)
19. F.X. Xiu, Z. Yang, L.J. Mandalapu, D.T. Zhao, J.L. Liu, Appl. Phys. Lett. **87**, 152101 (2005)
20. D. Gao, Y. Xu, Z. Zhang, H. Gao, D. Xue, J. Appl. Phys. **105**, 063903 (2009)
21. A.F. Kohan, G. Ceder, D. Morgan, C.G. Van de Walle, Phys. Rev. B **61**, 15019 (2000)
22. J.M.D. Coey, M. Venkatesan, C.B. Fitzgerald, Nat. Mater. **4**, 173 (2005)
23. J. Qi, Y. Yang, L. Zhang, J. Chi, D. Gao, D. Xue, Scr. Mater. **60**, 289 (2009)
24. Q. Wang, Q. Sun, G. Chen, Y. Kawazoe, P. Jena, Phys. Rev. B **77**, 205411 (2008)